

## Two-Step Condensation of the Ideal Bose Gas in Highly Anisotropic Traps

N. J. van Druten

*Huygens Laboratory, Leiden University, P.O. Box 9504, Leiden, The Netherlands*

Wolfgang Ketterle

*Department of Physics and Research Laboratory of Electronics, Massachusetts Institute of Technology, Cambridge, Massachusetts 02139*

(Received 10 March 1997)

The ideal Bose gas in a highly anisotropic harmonic potential is studied. It is found that Bose-Einstein condensation occurs in two distinct steps as the temperature is lowered. In the first step the specific heat shows a sharp feature, but the system still occupies many one-dimensional quantum states. In the second step, at a significantly lower temperature, the ground state becomes macroscopically occupied. It should be possible to verify these predictions using present-day atom traps. The two-step behavior can occur in a rather general class of anisotropic traps, including the box potential. [S0031-9007(97)03666-1]

PACS numbers: 03.75.Fi, 05.30.Jp, 32.80.Pj

The realization of Bose-Einstein condensation (BEC) in magnetically trapped, weakly interacting atomic gases [1] has revived interest in the theoretical study of the ideal Bose gas. Most textbooks, e.g., [2], calculate the behavior of the ideal Bose gas in a three-dimensional (3D) box, and then go to the thermodynamic limit. BEC is then characterized by a cusp in the specific heat at a finite temperature  $T_c$ , accompanied by a sudden onset of macroscopic ground-state population below  $T_c$ . The experiments deal with a limited number of atoms ( $N \lesssim 10^7$ ), and use traps that are approximately harmonic potentials. Hence recent theoretical efforts have concentrated on the influence of finite  $N$  for different trapping potentials and also on lower-dimensional systems [3–9], extending the earlier work of Refs. [10–12] (and references therein) which used the thermodynamic limit ( $N \rightarrow \infty$ ).

Those papers showed that the ideal Bose gas in an anisotropic 3D trap behaves very similarly to the isotropic case, the only difference being that the isotropic trap frequency is replaced by appropriate averages of the different trapping frequencies. The case of BEC in lower dimensions was understood as the limiting case of a 3D situation; when the temperatures of interest ( $\times k_B/\hbar$ ) are much smaller than the trapping frequencies in one or two dimensions, the dynamics in those dimensions are “frozen out” and the system behaves lower dimensionally. In the present paper, we show that BEC in anisotropic potentials is much richer.

The main new result is that for a highly anisotropic trap BEC happens in two steps as the temperature is lowered. In the first step, the particles condense into the ground state of the tightly confining dimension(s), while still occupying many quantum states in the weakly confining dimension(s). In the second step, at a significantly lower temperature, the overall ground state of the system suddenly develops a macroscopic occupation. This behavior shows general features of Bose-Einstein con-

den- sation which have not been emphasized before: When the temperature is lowered, the dimensionality of the system can be reduced not only by “freezing out” of degrees of freedom at temperatures comparable to the energy of the first excited state, but also by “Bose condensing to lower dimensions” at much higher temperatures. As a consequence, for a quite general class of potentials, BEC does not lead to a macroscopic population of the overall ground state (“single-mode condensate”), but results in the population of many states with respect to the weakly confining dimension (“multimode condensate”).

We explicitly demonstrate this behavior for the 3D harmonic trap. This case is the most relevant for experiments and is also mathematically convenient. Figure 1 summarizes our results. It shows how the two previously discussed regimes (normal 3D BEC and freezing out of motion) are separated by a regime where two-step BEC occurs. Two specific cases have been discussed before

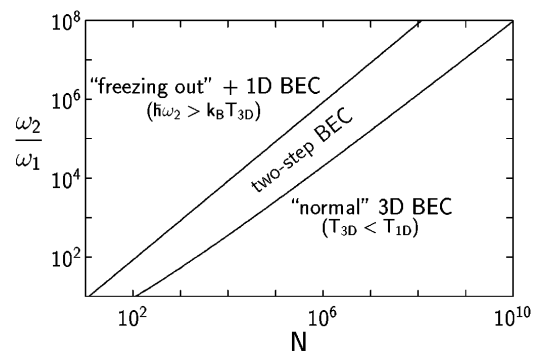


FIG. 1. Overview of the three different regimes of BEC in an anisotropic harmonic oscillator potential with  $\omega_1 \ll \omega_2 = \omega_3$ , as a function of particle number  $N$ , and trap anisotropy  $\omega_2/\omega_1$ . The regimes are separated by lines given by  $\hbar\omega_2 = k_B T_{3D}$  [upper line, see Eq. (8)], and  $T_{3D} = T_{1D}$  [lower line, see Eq. (7)], where  $T_{3D}$  and  $T_{1D}$  are the 3D and 1D condensation temperatures, respectively; see text.

where BEC into multiple states happens, the 2D rotating disk [11] and the gravito-optical trap [6]. Both papers dealt with limiting cases in which the second condensation step was absent. In contrast, we show here that the two-step behavior is a property of a rather general class of highly anisotropic traps, that it can persist in the thermodynamic limit, and that it should be experimentally realizable using current atom traps.

The ideal Bose gas is most conveniently described in the grand-canonical ensemble [2,13], in which the population  $N_i$  of a state with energy  $E_i$  is given by

$$N_i = \frac{ze^{-E_i/k_B T}}{1 - ze^{-E_i/k_B T}}, \quad (1)$$

where  $T$  is the temperature. Degeneracy factors are avoided by accounting for degenerate states individually. The fugacity  $z$  is determined by the constraint that the total number of particles be given by  $N = \sum_{i=0}^{\infty} N_i$ . This can be rewritten as

$$N(z, T) = \sum_{j=1}^{\infty} z^j \sum_{i=0}^{\infty} e^{-jE_i/k_B T}. \quad (2)$$

Once  $z$  has been determined, all thermodynamically relevant quantities can be calculated from partial derivatives of the grand potential  $q$ , the logarithm of the grand canonical partition function [2,7]. The specific heat  $C$  is obtained from  $C = (\partial U / \partial T)_N$  where  $U$  is the internal energy,  $U = \sum_i N_i E_i = k_B T^2 (\partial q / \partial T)_z$ . The grand potential  $q$  can be expressed as a sum similar to Eq. (2),

$$q(z, T) = \sum_{j=1}^{\infty} \frac{z^j}{j} \sum_{i=0}^{\infty} e^{-jE_i/k_B T}. \quad (3)$$

For the 3D harmonic trap the states can be labeled by three (non-negative integer) quantum numbers  $n_{1,2,3}$  corresponding to energies  $E_{n_1 n_2 n_3} = \hbar \sum_{d=1}^3 n_d \omega_d$ , where the energy of the ground state has been taken as zero. As a result, the sum over states in Eqs. (2) and (3) can be written as [4,7]

$$\begin{aligned} \sum_{i=0}^{\infty} e^{-jE_i/k_B T} &= \prod_{d=1}^3 \sum_{n_d=0}^{\infty} e^{-jn_d \epsilon_d} \\ &= \prod_{d=1}^3 \frac{1}{1 - e^{-j\epsilon_d}}, \end{aligned} \quad (4)$$

where we have defined  $\epsilon_d = \hbar \omega_d / k_B T$ . For reasonable  $N$  (say  $N < 10^6$ ) it is now feasible to evaluate Eqs. (2) and (3) numerically, after the ground-state contribution  $N_0 = g_0(z) = z/(1-z)$  and  $q_0 = g_1(z) = -\ln(1-z)$  has been split off. Here the Bose functions  $g_n(z)$  are defined as usual by  $g_p(z) = \sum_{j=1}^{\infty} z^j / j^p$  [2].

The solid lines in Fig. 2(a) show the exact results for an ideal Bose gas of  $10^6$  particles in a highly anisotropic 3D harmonic trap with tight radial and weak axial confinement. For comparison, Figs. 2(b) and 2(c) show, respectively, the well-known behavior in a 3D isotropic trap [3,4,10,12], and in a 1D harmonic trap [4,5,8,9] for the same number of particles.

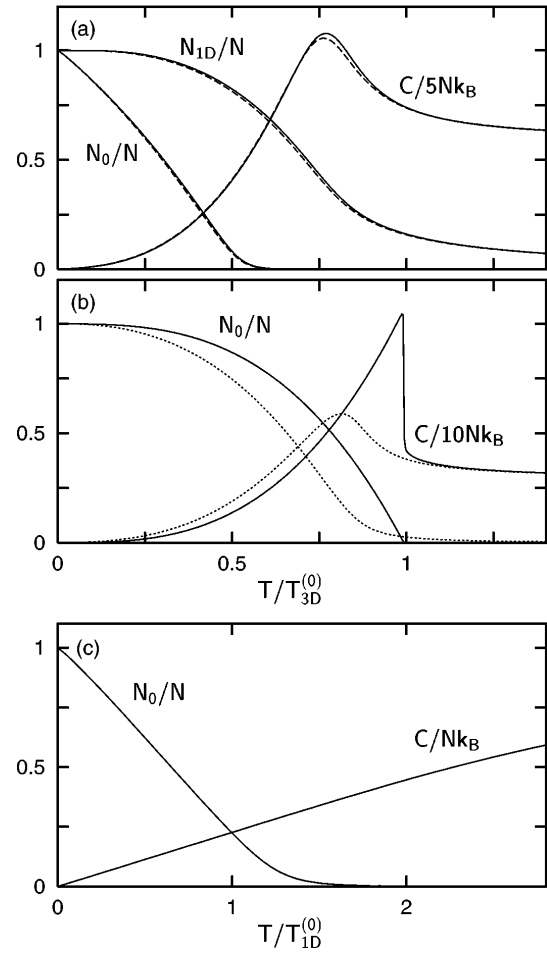


FIG. 2. The behavior of an ideal Bose gas in a harmonic trap with  $N = 10^6$  particles (solid lines). (a) 3D highly anisotropic trap,  $\omega_2 = \omega_3 = 5.6 \times 10^4 \omega_1$ , corresponding to  $T_{3D}^{(0)} = 2T_{1D}^{(0)}$ . (b) 3D isotropic trap  $\omega_1 = \omega_2 = \omega_3$ . (c) 1D trap  $\hbar \omega_1 \ll k_B T \ll \hbar \omega_{2,3}$ . The ground-state fraction  $N_0/N$  and specific heat per particle  $C/Nk_B$  are plotted. In (a), the fraction of the population that is excited in the  $\omega_1$  direction only,  $N_{1D}/N$ , is also plotted. The dashed lines in (a) were calculated using Eq. (6); in (b) and (c) this approximation is indistinguishable from the exact result. The dotted line in (b) shows how the 3D condensation smooths and shifts for low particle number ( $N = 10^2$ ).

Clearly, the behavior in the highly anisotropic trap is qualitatively different from that in an isotropic trap or in 1D. In fact, Fig. 2(a) combines the features of Figs. 2(b) and 2(c) in an interesting way. As the temperature is lowered, condensation occurs in two steps. First, the specific heat per particle increases from the temperature-independent classical-gas value, shows a maximum and then a rapid decrease, as in the 3D isotropic case (and unlike the 1D case). Unlike the 3D isotropic case, however, this is not accompanied by a sudden increase of the ground-state fraction. Instead, the population that is excited in the direction of  $\omega_1$  only,  $N_{1D} = \sum_{n_1=0}^{\infty} N_{n_1,0,0}$ , increases rapidly, as shown in Fig. 2(a) [the nonzero value of  $N_{1D}$  at higher temperatures is a finite- $N$  effect, see Figs. 2(b) and 3]. The ground-state fraction becomes significant only in

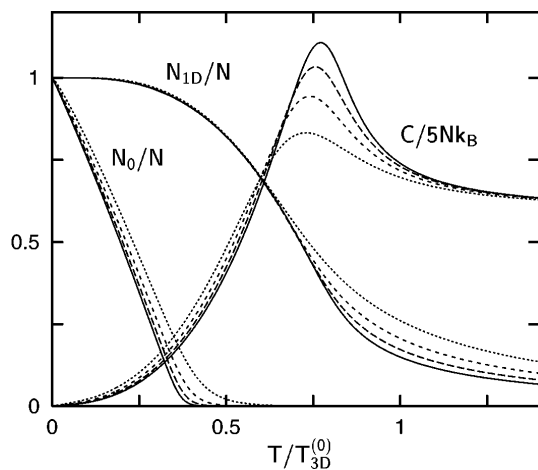


FIG. 3. Behavior of the ideal Bose gas in a harmonic trap with  $\omega_1 \ll \omega_2 = \omega_3$  for a different particle number,  $N = 10^4$  (dotted),  $10^6$  (short dashed),  $10^8$  (long dashed), and  $10^{10}$  (solid lines). The condensation temperatures were kept fixed,  $T_{3D}^{(0)} = 3T_{1D}^{(0)}$ , see text. Shown are the ground-state fraction,  $N_0/N$ , the fraction of the population excited in the  $\omega_1$  direction only,  $N_{1D}/N$ , and specific heat per particle,  $C/Nk_B$ .

the second step at lower temperatures, and increases approximately linearly with decreasing temperature, without a feature in the specific heat, as in the 1D case.

The behavior shown in Fig. 2 can be quantitatively understood using a simple, yet powerful approximation scheme. First, we note that the series appearing in Eq. (4) can be written as

$$\sum_{n=0}^{\infty} e^{-nx} = 1 + \frac{e^{-x\alpha(x)}}{x}. \quad (5)$$

This corresponds to splitting off the ground-state contribution for each excitation direction. The function  $\alpha(x)$  defined implicitly in Eq. (5) depends only weakly on  $x$  ( $x > 0$ ),  $1/2 < \alpha < 1$ . For small  $x$ , one has  $\alpha = 1/2 + x/24$ ; since the second term on the right-hand side of Eq. (5) is only significant for small  $x$ , setting  $\alpha = 1/2$  is a very good approximation [4], with a maximum relative error of 2.5% [15]. Inserting this into Eqs. (2) and (3) yields

$$N(z, T) = g_0(z) + \left[ \frac{1}{\epsilon_1 \epsilon_2} g_2(z e^{-(\epsilon_1 + \epsilon_2)/2}) + \text{c.p.} \right] + \frac{1}{\epsilon_1 \epsilon_2 \epsilon_3} g_3(z e^{-(\epsilon_1 + \epsilon_2 + \epsilon_3)/2}) + \left[ \frac{1}{\epsilon_1} g_1(z e^{-\epsilon_1/2}) + \text{c.p.} \right], \quad (6)$$

and the same expression for  $q(z, T)$ , but replacing every  $g_p$  by  $g_{p+1}$ . Here c.p. denotes terms that are obtained by cyclic permutation of  $\epsilon_1$ ,  $\epsilon_2$ , and  $\epsilon_3$  (e.g.,  $[\epsilon_1 \epsilon_2 + \text{c.p.}] \equiv \epsilon_1 \epsilon_2 + \epsilon_2 \epsilon_3 + \epsilon_3 \epsilon_1$ ). Similar approximate expressions have been derived using the Euler-Maclaurin summation [8] and the Barnes zeta function [7]. The above derivation is appealing because of its simplicity and because it yields direct physical insight into the meaning of each term

in Eq. (6): Each  $g_p$  corresponds to the population of states that are excited in  $p$  directions. The  $\epsilon_d$ 's that appear in the exponents and as prefactors indicate the excitation directions involved. Results obtained with this approximation are shown as dashed lines in Fig. 2, and are almost indistinguishable from the exact results.

To explain the behavior in Fig. 2(a) it is useful to first explain Figs. 2(b) and 2(c) starting from Eq. (6). For the 3D isotropic harmonic trap [Fig. 2(b)],  $k_B T \gg \hbar \omega_{1,2,3}$ , so that all  $\epsilon_d \ll 1$ . Thus, the  $g_3$  term in Eq. (6) dominates over the  $g_1$  and  $g_2$  terms. Physically, this means that the excited-state population is dominated by states that are excited in all three directions. Since the argument of the  $g_3$  function is smaller than 1, the excited-state population cannot exceed  $g_3(1) (k_B T / \hbar)^3 / (\omega_1 \omega_2 \omega_3)$  [ $g_3(1) \approx 1.202$ ]. This is the basis of Bose-Einstein condensation: When the temperature is lowered, the excited-state population will “saturate” at the above value, and the excess particles present will “condense” into the ground state. The “condensation temperature”  $T_{3D}$  is approximately given by  $T_{3D}^{(0)} \equiv (\hbar/k_B) [N \omega_1 \omega_2 \omega_3 / g_3(1)]^{1/3}$ , and corresponds to a situation where approximately one state per particle is thermally accessible.

For the 1D case shown in Fig. 2(c),  $\epsilon_1 \ll 1 \ll \epsilon_{2,3}$ , and the excited-state population is dominated [in Eq. (6)] by the  $g_1$  term involving  $\epsilon_1$ . As in the 3D case, this population has an upper bound, and thus one can define a 1D condensation temperature  $T_{1D}$  by  $N = (k_B T_{1D} / \hbar \omega_1) \ln(2k_B T_{1D} / \hbar \omega_1)$  [4,9]. Although the specific heat does not show a feature at  $T_{1D}$ , the condensate fraction does show a sudden onset for large  $N$  at  $T_{1D}$  [4], which is  $\approx \ln(2N)$  times lower than the temperature where approximately one state per particle is thermally accessible. As a consequence, in the usual thermodynamic limit in  $d$  dimensions ( $N \rightarrow \infty$ , with  $N \prod_{i=1}^d \omega_i$  kept constant) [10,12], the 1D condensation temperature vanishes, in contrast to the 3D condensation temperature.

These observations are useful for explaining the behavior in highly anisotropic traps. The behavior shown in Fig. 2(a) results when  $T_{3D} > T_{1D}$ : At  $T_{3D}$  the 3D-excited-state population saturates, leading to the peak in the specific heat. Unlike the usual case, however, upon lowering the temperature, the excess particles do *not* necessarily condense into the ground state, since the 1D population is not saturated yet. Thus the excess particles first condense into the states which are excited in one direction only. Upon further lowering the temperature,  $T_{1D}$  is reached, and the excess particles condense into the ground state, similar to a 1D Bose gas. Thus one simple equation [Eq. (6)] explains the two-step behavior as well as finite- $N$  effects in arbitrary dimensions.

We now discuss quantitatively the conditions for two-step BEC. In order to keep the following equations as simple as possible, we approximate  $T_{3D}$  by  $T_{3D}^{(0)}$  and  $T_{1D}$  by  $T_{1D}^{(0)} \equiv N \hbar \omega_1 / k_B \ln(2N)$ ; both approximations are

accurate to within 20% for the cases we consider here. For a trap with  $\omega_1 \ll \omega_2 = \omega_3$ , the condition  $T_{1D}^{(0)} < T_{3D}^{(0)}$  can be rewritten as

$$N[g_3(1)]^{1/2}[\ln(2N)]^{-3/2} < \omega_2/\omega_1. \quad (7)$$

This shows explicitly that highly anisotropic traps are needed. In addition, 3D Bose condensation requires  $\hbar\omega_2 < k_B T_{3D}$ , or

$$\omega_2/\omega_1 < N g_3(1), \quad (8)$$

otherwise the first step is freezing out of the motion in the direction of  $\omega_2$  and  $\omega_3$ . This is fulfilled when  $N$  is sufficiently large. The softening of the transition due to finite- $N$  effects is enhanced by the anisotropy because the ratio  $\hbar\omega_2/k_B T_{3D}$  is increased [see also Fig. 2(b)].

Figure 3 shows the behavior of the ideal Bose gas for several  $N$ , keeping  $T_{1D}^{(0)}$  and  $T_{3D}^{(0)}$  fixed (with  $T_{3D}^{(0)} = 3T_{1D}^{(0)}$ ). As  $N$  is increased both features become increasingly sharp. Note that keeping  $T_{3D}^{(0)}$  fixed as  $N \rightarrow \infty$  corresponds to the usual thermodynamic limit in 3D. The condition that  $T_{1D}^{(0)}$  be kept fixed imposes an additional constraint; it defines the anisotropy of the trap, which is left unspecified in the usual thermodynamic limit.

As is evident from the discussion above, the two-step behavior can occur because, unlike  $T_{3D}$ ,  $T_{1D}$  is much lower than predicted by the ‘‘one particle per thermally accessible quantum state’’ criterion [due to the  $\ln(2N)$  term in  $T_{1D}^{(0)}$ ]. This is what allows the condition  $T_{1D} < T_{3D}$  to be fulfilled while maintaining the high-temperature condition. Two-step Bose condensation will therefore not occur for  $\omega_1 = \omega_2 \ll \omega_3$ . Using the results from Ref. [12], it can be stated more generally that two-step condensation is possible when the full-dimensional system shows BEC within the continuous-spectrum approximation, while the lower-dimensional system does not. Many of the power-law traps considered in Ref. [12] have this property.

An important example is the 3D box. The excited-state population in a  $d$ -dimensional box is described by  $g_{d/2}$ . For a box with size  $L_1 \times L_2 \times L_3$  the 3D condensation temperature is given by  $N = (L_1 L_2 L_3 / \Lambda_t^3) g_{3/2}(1)$  [2], while for the 2D box with size  $L \times L$  it follows from  $N = 2(L/\Lambda_t)^2 \ln(L/\Lambda_t)$  [4], with  $\Lambda_t$  the thermal de Broglie wavelength. As a consequence, for a box with  $L_1 \ll L_2 = L_3$ ,  $T_{3D}^{\text{box}} > T_{2D}^{\text{box}}$  if  $L_2/L_1 > g_{3/2}(1)N^{1/2}[\ln(N)]^{-3/2}$ , a condition which can be satisfied while maintaining the high-temperature condition  $\Lambda_t < L_{1,2,3}$  if  $N$  is sufficiently large. A 3D box satisfying these conditions will show similar two-step condensation as in Fig. 3, with the peak in specific heat occurring at  $T_{3D}^{\text{box}}$ , and the onset of macroscopic ground-state population occurring at  $T_{2D}^{\text{box}}$ . For  $L_1 \ll L_2 \ll L_3$  we expect even three-step behavior because the condensation temperature for the 1D box with size  $L$  is given by  $N = (\pi/3)(L/\Lambda_t)^2$ .

The two-step BEC discussed here should be experimentally observable using currently available atom traps. An anisotropy of  $\omega_2 = \omega_3 = 1000\omega_1$  should be achievable in magnetic traps of the Ioffe-Pritchard type and in optical dipole traps [4]. With  $N = 10^4$  atoms, one could realize  $T_{3D}^{(0)} = 2T_{1D}^{(0)}$ . The experimental signature would be a sudden decrease of the spatial and velocity distributions first radially at  $T_{3D}$  and then axially at  $T_{1D}$ .

We thank H. Wallis and D.M. Kurn for discussions. N.J.vD.’s work is part of the research program of the ‘‘Stichting voor Fundamenteel Onderzoek der Materie (FOM)’’ and was made possible by the financial support of NWO. W.K. acknowledges ONR, NSF, ARO (JSEP), and the Packard foundation for financial support.

*Note added.*—After submission of this work, we learned that the results for the 3D anisotropic box potential were found before by Sonin [16]. We thank G. Shlyapnikov for bringing this paper to our attention.

- 
- [1] M.H. Anderson *et al.*, *Science* **269**, 198 (1995); K.B. Davis *et al.*, *Phys. Rev. Lett.* **75**, 2909 (1995); C.C. Bradley, C.A. Sackett, and R.G. Hulet, *Phys. Rev. Lett.* **78**, 985 (1997).
  - [2] K. Huang, *Statistical Mechanics* (Wiley, New York, 1987), 2nd ed.
  - [3] S. Grossmann and M. Holthaus, *Phys. Lett. A* **208**, 188 (1995); *Z. Phys. A* **50**, 323 (1995); **50**, 921 (1995); *Z. Phys. B* **97**, 319 (1995).
  - [4] W. Ketterle and N.J. van Druten, *Phys. Rev. A* **54**, 656 (1996).
  - [5] S. Grossmann and M. Holthaus, *Phys. Rev. E* **54**, 3495 (1996).
  - [6] H. Wallis, *Quantum Semiclass. Opt.* **8**, 727 (1996).
  - [7] K. Kirsten and D.J. Toms, *Phys. Lett. A* **222**, 148 (1996); *Phys. Rev. A* **54**, 4188 (1996).
  - [8] (a) H. Haugerud, T. Haugset, and F. Ravndal, *Phys. Lett. A* **225**, 18 (1997); (b) T. Haugset, H. Haugerud, and J.O. Andersen, *Phys. Rev. A* **55**, 2922 (1997).
  - [9] W.J. Mullin, *J. Low Temp. Phys.* **106**, 615 (1997).
  - [10] S.R. de Groot, G.J. Hooyman, and C.A. ten Seldam, *Proc. R. Soc. London A* **203**, 266 (1950).
  - [11] J.J. Rehr and N.D. Mermin, *Phys. Rev. B* **1**, 3160 (1970).
  - [12] V. Bagnato, D.E. Pritchard, and D. Kleppner, *Phys. Rev. A* **35**, 4354 (1987); V. Bagnato and D. Kleppner, *Phys. Rev. A* **44**, 7439 (1991).
  - [13] It has been found that, for the quantities presented here, the differences between grand-canonical, canonical, and microcanonical ensembles are small, see Refs. [5,8(b),14], and H.D. Politzer, *Phys. Rev. A* **54**, 5048 (1996).
  - [14] C. Herzog and M. Olshanii, *Phys. Rev. A* **55**, 3254 (1997).
  - [15] Equation (5) is an excellent and controlled approximation for the whole regime, but it is not a systematic mathematical expansion. For high temperatures ( $\epsilon \ll 1$ ), it correctly gives the two leading terms for 3D BEC. For 1D and  $z = 1$ , it gives  $N - N_0 = (1/\epsilon)[\ln(1/\epsilon) + \ln(2)]$ , whereas the exact result has the Euler constant instead of  $\ln(2)$ .
  - [16] E.A. Sonin, *Sov. Phys. JETP* **29**, 520 (1969).